

Stress Concentration and Stability Studies in Composite Ribs with flanged cutouts

Paper Reference Number: 2001-136

Ruchin Pandey, Sandeep Thakur and Ramanath KS,
CAE Group, Infosys Technologies Limited, Bangalore, India.
(ramanath_ks@infy.com)

Prof. K.P. Rao,
Dept. of Aerospace Engg, Indian Institute of Science, Bangalore, India
(aerokp@aero.iisc.ernet.in)

Abstract:

Carbon reinforced composites (CFC) or Carbon Fiber Reinforced Plastics (CFRP) are used extensively in aircraft structures as they give high stiffness and strength with lower weight. Typical composite components of aircraft are wings, empennage and parts of fuselage. Wing ribs and intermediate spars are typical sub-structures, which can be built of CFC. Cutouts are introduced in these structures for lightening the component. Introduction of holes leads to stress concentrations as also lowering of the buckling load carrying ability. Reinforcement of holes is necessary to reduce stresses in the vicinity of the hole and also to enhance the buckling loads.

In this paper we consider a shear loaded square panel representing a segment of a composite (T300/914C) rib containing a reinforced circular cutout. Flanged holes considered are similar to those present in typical aluminum ribs and spars. A study of the effect of various reinforcement parameters is made both on strength and stability using MSC.Nastran. Studies show that use of CFC in such situations leads to weight savings.

Keywords:

Nastran, Stress Concentration, Stability, Composites, Rib

(Paper accepted in the 2001 World MSC. Aerospace Conference Toulouse, France, Sept 24-26, 2001)

Introduction:

Improvement in flight performance is one of the most important criteria in the design of aerospace structures. Weight reduction measures, coupled with compliance to strength, stiffness and stability requirements are important. Investigators have long been in search of materials that have less weight as well as sufficient strength and stiffness to withstand aerodynamic loads experienced by a structure in various flight conditions. Fiber reinforced composite materials have been found to have promising properties in this regard. These materials are being used extensively in the production of various aircraft components and their usage is increasing day-by-day. This is due to the fact that they have a very high strength-to-weight ratio, higher damage tolerance, better manufacturability and lesser number of joints compared to conventional materials. The applicability and performance of composites in a typical composite aircraft rib / spar with flanged cutouts is studied in this paper.

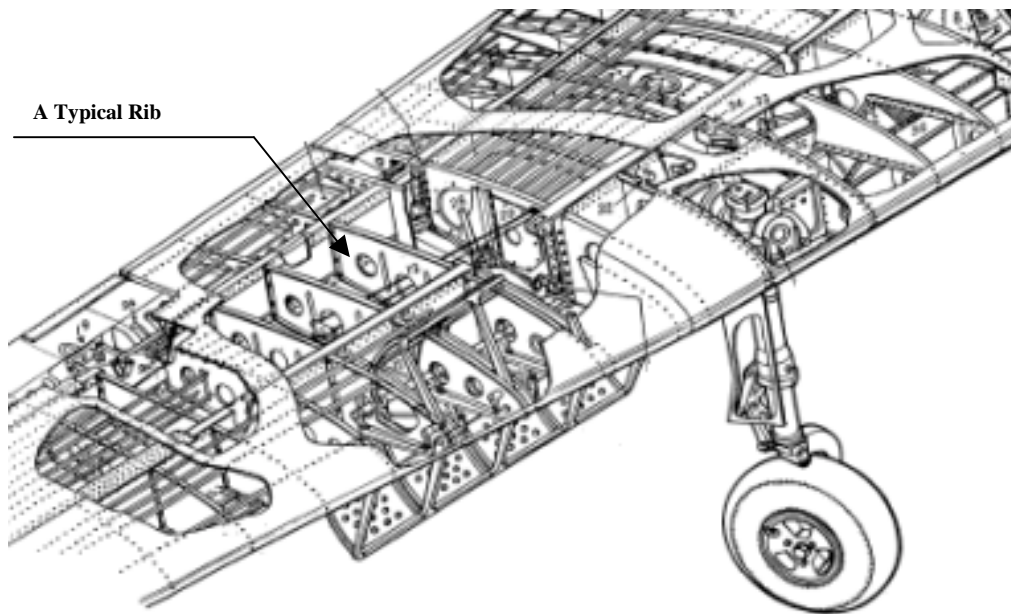


Fig. 1. A typical aircraft wing illustrating the rib configurations

Problem Definition:

A typical aircraft wing is shown in fig 1. It consists of skins, longitudinal spars for providing bending stiffness and transverse ribs to take any transverse load. Cutouts are provided in the ribs for the passage of the fuel stored in the wing and for weight reduction. Stress concentration occurs around any cutout in a loaded plate. To alleviate this effect, one has to adopt various schemes of reinforcement. Some methods of reinforcement feasible from the manufacturing point of view are as shown in fig 2. A reinforcement ratio (μ), indicative of the weight saved is defined as the ratio of the weight of reinforcement to the weight of sheet cut.

In the present work, the effect of utilization of Carbon Fiber Reinforced Plastic (CFRP) in lieu of Aluminum on the stress concentration factor (SCF) and the buckling load factor (BLF) in a typical rib is studied.

Analysis:

A S.S. plate of size of 300 mm X 300 mm X 2 mm is used in the study. A uniform in-plane shear loading of 20 N/mm along all the outer edges is considered in the analysis. MSC.Nastran V70.7 and MSC.Patran 2000 are used for the FE Analysis [4]. The analysis is carried out in three steps, which are detailed below:

(i) Validation study:

Validation study for element selection, boundary conditions, loading conditions and modeling is carried out for estimating SCF and BLF in aluminum alloy as well as CFRP plates. The aluminum alloy is henceforth referred to as “isotropic material”. It has the following material properties:

$$E=70000 \text{ MPa}; \nu=0.3; \rho = 2.7 \text{ g/cc.}$$

The Composite Material used is T300/914C and it has the following material properties:

$$E_{11}=130000 \text{ MPa}; E_{22}=10000 \text{ MPa}; \nu_{12}=0.35; G_{12}=5000 \text{ MPa}; \\ G_{23}= 3270 \text{ MPa}; G_{13}= 5000 \text{ MPa}; X_t = 1200 \text{ MPa}; X_c = 1000 \text{ MPa}; Y_t = 40 \text{ MPa}; \\ Y_c = 246 \text{ MPa}; S = 65 \text{ MPa}; \rho = 1.8 \text{ g/cc.}$$

(ii) Study of a typical configuration:

A typical configuration (fig. 2) of an aircraft rib segment with reinforced cutout is selected. The laminate used has 16 layers each of 0.125 mm thickness and is symmetrically laid across mid-plane with a stacking sequence of $[-45/45/-45/45/-45/45/-45/45]_s$. This material is referred to as “composite material” henceforth. Comparative analysis is carried out for shear loading for isotropic and composite material. The SCF and the BLF are obtained for configurations 1 through 4 (fig. 2). The meshing of the models is based on the observations of the validation phase.

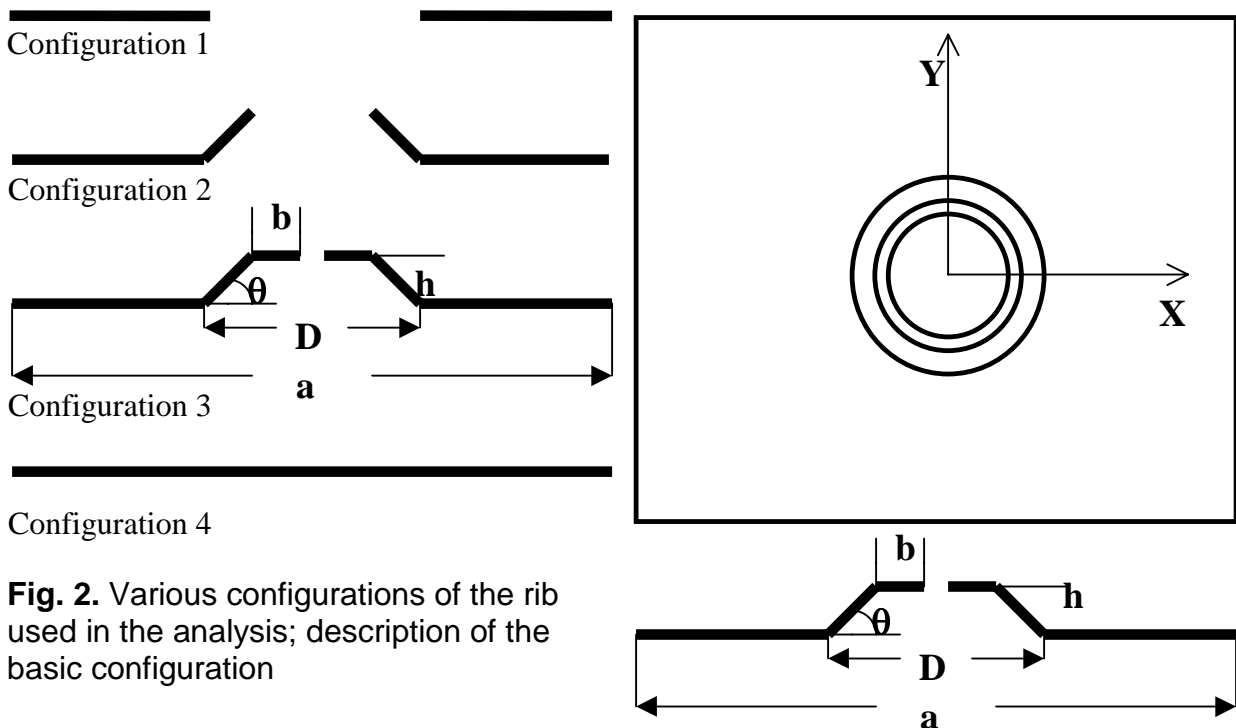


Fig. 2. Various configurations of the rib used in the analysis; description of the basic configuration

(iii) Parametric Studies:

The effect of variation in flange height for various cutout diameters on the SCF and the BLF is studied for the basic configuration (fig. 2) using composite material. Also, Tsai-Wu failure criterion is applied and the failure indices are calculated for all the configurations.

In configuration 4, uniform meshing is used while in all other cases; the density of elements is more near the periphery of the hole as it is the region of high stress gradient. The graded mesh has been arrived at by analysis iterations for convergence.

Results and Discussions:

(i) Validation Study:

An isotropic square plate of size 300 mm X 300 mm X 2 mm with 20 mm diameter cutout is used for the validation of element formulation, mesh density, etc. Four different meshing schemes are used for this purpose under uni-axial tension, bi-axial tension and shear loading. The result of this analysis is shown in Table 1. It is found that with scheme No. 2, the SCF comes out to be 2.987 for uni-axial loading, which has less than 1% error [1]. For composite material, the validation for SCF is done by comparing the results with theory of Lekhnitskii [2]. A uni-directional orthotropic laminate is subjected to uni-axial tension along the fiber. Good agreement is observed.

Table 1. Meshing Schemes used and the SCF obtained

Meshing Scheme No.	Element Geometry	No. of elements along cutout circumference	Loading	SCF (Present)	SCF (Analytical) [Ref. 1]
1	CQUAD4	32	Uni-axial	2.878	3.00
2	CQUAD4	64	Uni-axial	2.987	3.00
3	CQUAD8	32	Uni-axial	2.956	3.00
4	CQUAD8	64	Uni-axial	2.998	3.00
2	CQUAD4	64	Bi-axial	2.011	2.00
2	CQUAD4	64	Shear	3.898	4.00

The validation for BLF prediction is done by using both isotropic and orthotropic square plates of 10 mm X 10 mm X 0.096 mm and comparing the results with the analytical solutions (Table 2) obtained by Chamis [3]. This study indicates that 4-noded iso-parametric quadrilateral shell element together with meshes (Scheme 2) used, yields converged results for this problem.

Table 2. BLF Predictions using Scheme 2

Loading	Comparison of BLF	Isotropic	Orthotropic (0 Deg)
N_x / N_{cr}	Chamis [3]	1.000	1.000
	Present	0.997	0.993
N_{xy} / N_{cr}	Chamis [3]	1.000	1.000
	Present	0.987	0.984

(ii) Plate with a Flanged Hole (Typical Configuration):

The actual problem of rib segment is tackled maintaining the same type of mesh and the boundary conditions used for the validation. All configurations (from 1 to 4 of Fig. 2) are analyzed. The FE Mesh plot for a typical configuration of Rib with reinforcement is shown in Fig. 3

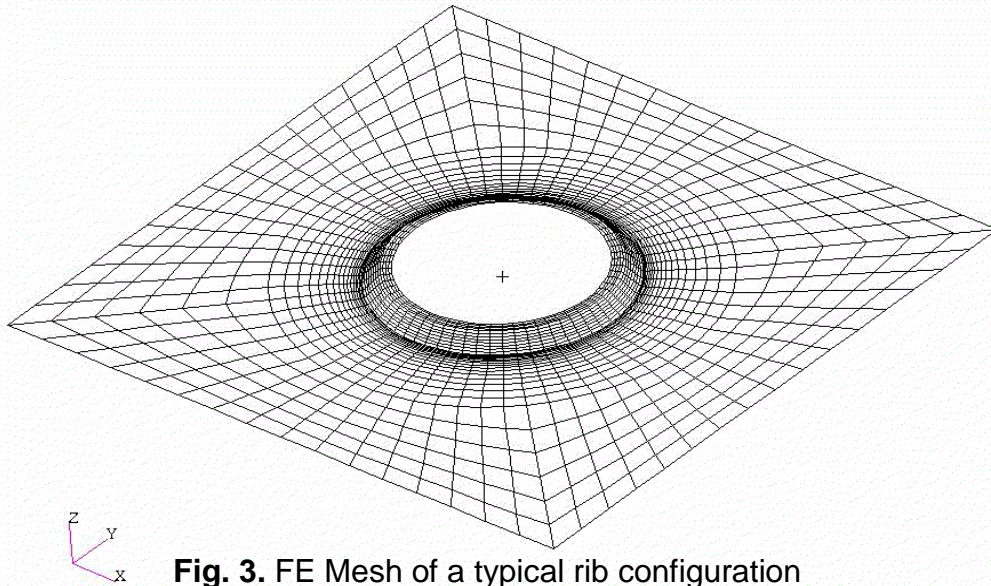


Fig. 3. FE Mesh of a typical rib configuration

SCF:

For configurations 1, 2 and 3, the SCF for a 60-mm cutout is calculated for both isotropic as well as composite rib under a uniform shear load of 20 N/mm. The results are tabulated below in table 3 and table 4.

Table 3. Stress Concentration factors for different flanged hole of isotropic rib

Configuration	b (mm)	h (mm)	θ ($^{\circ}$)	Reinforcement Ratio (μ)	Weight (kg)	SCF
1	0	0	0	0	0.471	4.40
2	0	8	45	0.652	0.481	2.38 (Lower) 4.01 (Upper)
3	5	8	45	0.868	0.484	2.10 (Lower) 4.16 (Upper)

Table 4. SCF for different flanged hole of composite rib

Configuration	b (mm)	h (mm)	θ ($^{\circ}$)	Reinforcement Ratio (μ)	Weight (kg)	S.C.F.
1	0	0	0	0	0.314	11.08
2	0	8	45	0.652	0.320	9.02
3	5	8	45	0.868	0.323	9.03

For the isotropic case, SCF decreases with increase in reinforcement. Also, SCF for the upper and lower layers are significantly different in the case of reinforced plates, which can be attributed to the stretching-bending coupling. Thus the tensile stresses in upper surface are higher compared to the bottom surface.

The SCF values are larger in the composite rib than the isotropic rib in a particular layer as is clear from table 4. This is due to the combined effect of material orthotropy, lay-up sequence, eccentricity and the compatibility requirement. Also, there is a small deleterious effect of reinforcement on the SCF. In fact, the SCF increases slightly due to reinforcement in the composite plate. This increase in the stress can be attributed to the orthotropic nature of the material, which along with the asymmetric shape of the rib with respect to the middle plane causes coupling effects, which increases the stress value. Fig. 4, 5 and 6 give principal stress distributions for the isotropic and composite cases.

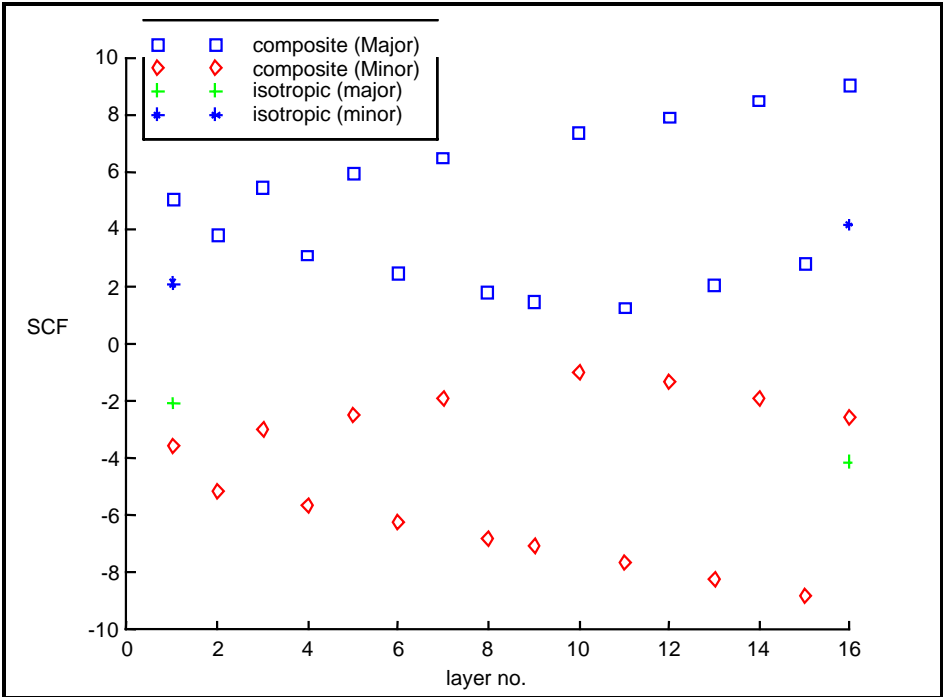


Fig. 4. Layer-wise Major and Minor Principal SCF of the Basic Configurations for Composite and Isotropic Rib

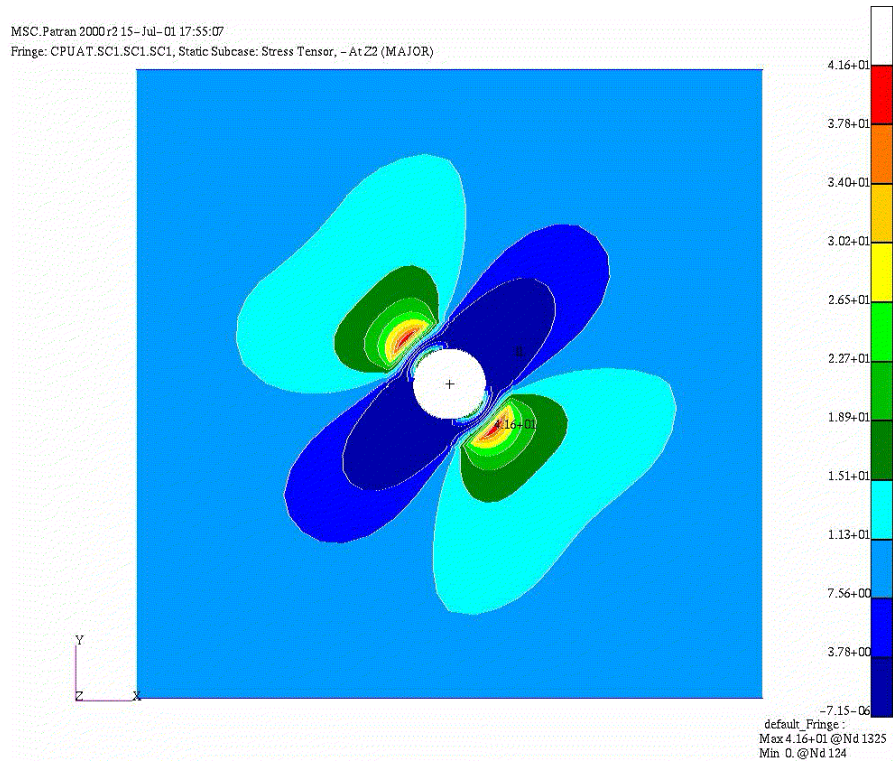


Fig. 5. Fringe plot of SCF for isotropic rib

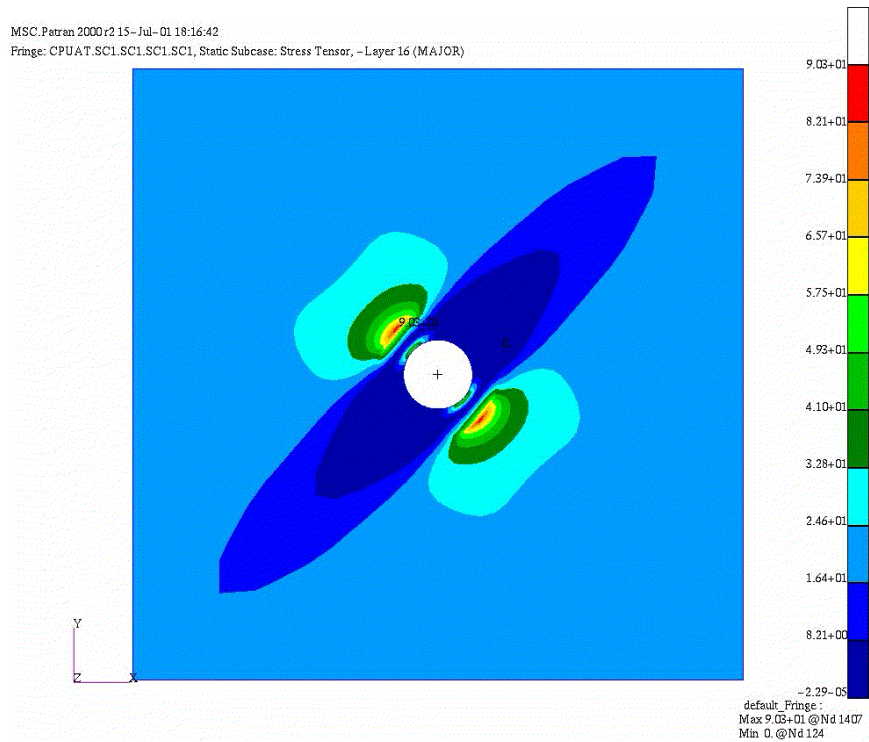


Fig. 6. Fringe plot of SCF for composite rib

To get a feel of how stresses vary near the bends in the reinforcement, a plot is shown in fig. 7. Here station numbers 1 to 5 indicate the end zones of cutout, flange and the lip respectively.

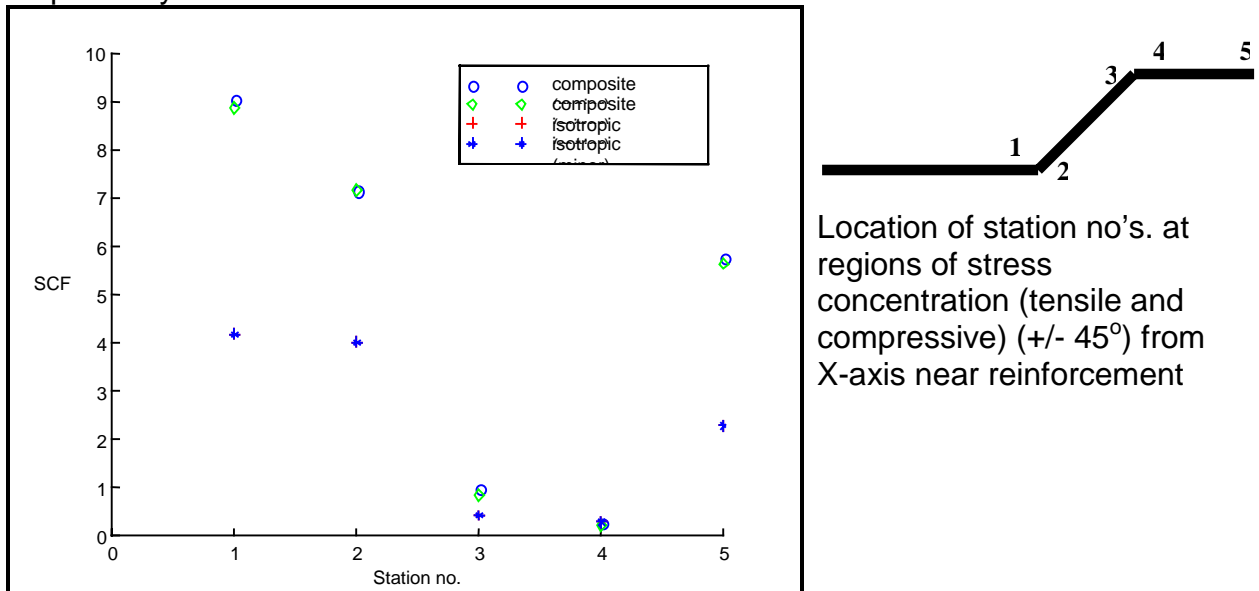


Fig. 7. SCF at various stations in the typical configuration for Composite and isotropic Rib.

Buckling:

For all the 4 configurations, the BLF are determined for both isotropic and composite ribs. The BLF for the first mode are tabulated in tables 5 and 6. Typical mode shapes are given in Figs. 8 – 11.

Table 5. Buckling Load Factors for isotropic rib (Shear Flow = 20 N/mm)

Configuration	b (mm)	h (mm)	θ (°)	Reinforcement Ratio (μ)	BLF (for mode 1)
1	0	0	0	0	1.949
2	0	8	45	0.652	2.689
3	5	8	45	0.868	2.850
4	-	-	-	-	2.650

It is clear from the tables that the BLF increases with addition of the reinforcement for both the isotropic as well as the composite rib. It is interesting to note that the BLF for configurations 2 and 3 is greater than the plate without cutout. This can be attributed to the fact that the reinforcement results in the reduction in the effective aspect ratio of the plate. It can be observed that successive buckling modes (for example, mode-1 and mode-2), for the isotropic rib, are symmetric while it is not true for the composite rib. This difference can be attributed to the orthotropic nature of the composite material and the presence of bending-twisting coupling existing in the laminate.

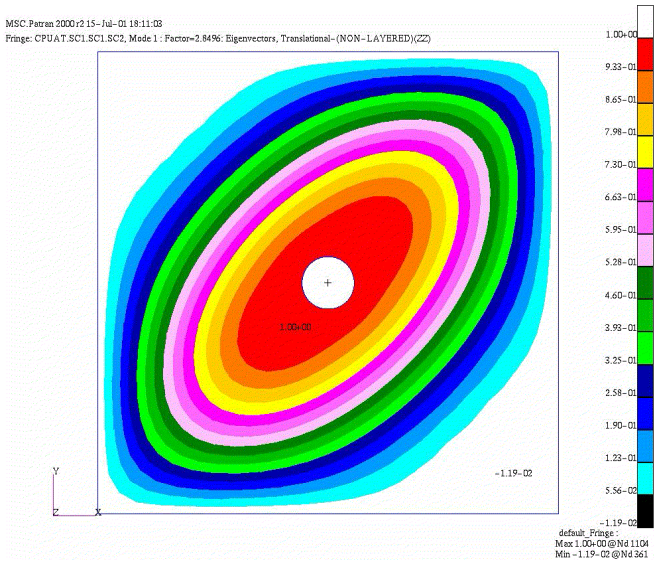


Fig. 8. Mode 1 for isotropic rib

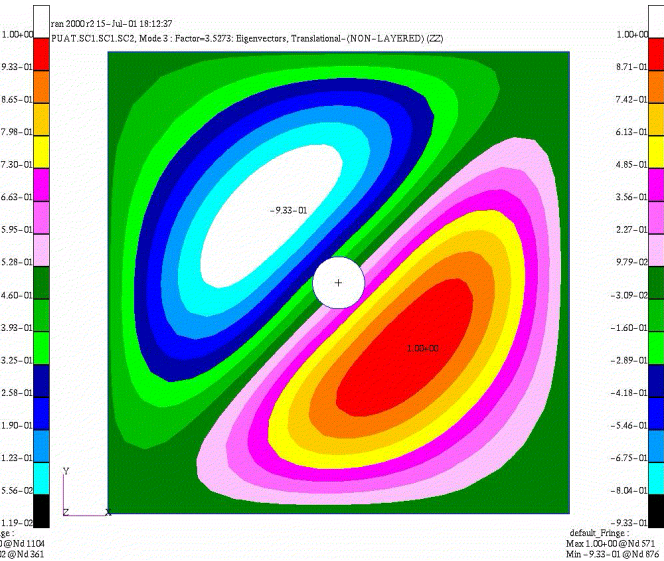


Fig. 9. Mode 3 for isotropic rib

Table 6. Buckling Load Factor for Composite Plate (Shear Flow = 20 N/mm)

MODE NO.	Config. 1 (with $D=60$)	Config. 2 (with $D=60$)	Config. 3 (with $D=60$)	Config. 4 (Flat Plate)
1	1.490	2.011	2.147	2.010
2	-1.903	2.418	2.432	2.280
3	2.219	-2.469	-2.666	-2.545
4	-2.841	-3.093	-3.143	-2.895
5	3.359	4.295	4.442	5.025
6	-4.209	-5.294	-5.472	5.440
7	4.749	5.455	5.857	6.055
8	4.856	5.476	5.906	6.170
9	5.015	5.731	5.925	-6.435
10	-6.066	-6.894	-7.390	-6.695

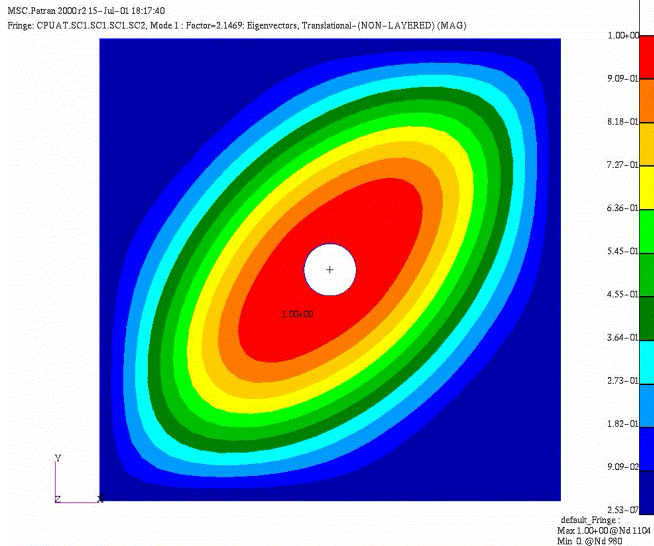


Fig. 10. Mode 1 for Composite Rib

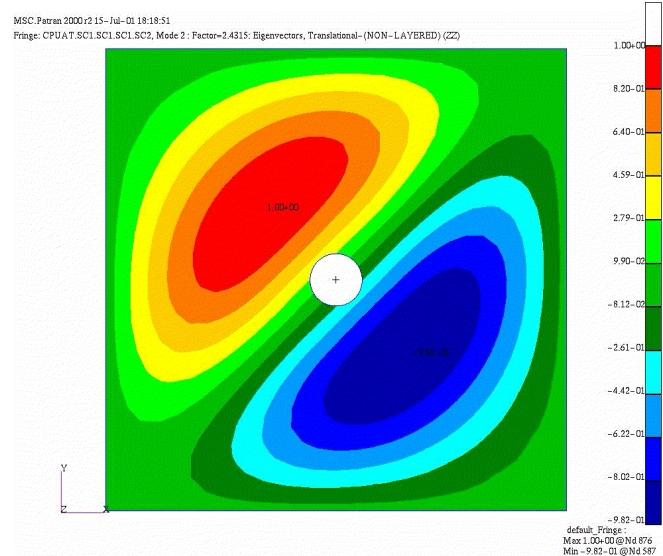


Fig. 11. Mode 2 for Composite Rib

(iii). Parametric Study:

Parametric study is carried out for various values of μ for configuration 3. Even though the lip is not giving large dividend, it is required to avoid de-lamination at the end of flange and from other manufacturing considerations. Three different cutout diameters: 60mm, 90mm and 120mm are studied for three different values of flange height 'h' (4mm, 6mm and 8mm). The lip width and flange angle is kept constant at 5mm and 45° respectively for all the cases. SCF values and Tsai-Wu failure indices (for strength evaluation) for various values of D and h are tabulated in table 7. BLF for a shear flow of 20 N/mm is given in table 8.

Table 7. SCF values for various cutout sizes of the composite rib

Sl. No.	D (mm)	h (mm)	Reinforcement Ratio (μ)	SCF	Tsai-Wu Failure Indices
1	60	4	0.612	10.47	0.170
2	60	6	0.746	9.29	0.164
3	60	8	0.868	9.03	0.160
4	90	4	0.430	12.50	0.216
5	90	6	0.531	11.64	0.204
6	90	8	0.627	11.04	0.194
7	120	4	0.330	16.40	0.287
8	120	6	0.411	14.40	0.264
9	120	8	0.488	14.30	0.254

Note: 16th layer is the topmost layer and SCF is maximum for major principal stress

SCF: It is clear from table 7, that increase in h results in a decrease in SCF but the gain is not very significant. It is also evident that the SCF value increases with the increase in cutout diameter, which is in accordance with the classical theory. The increase in the value of SCF with cutout diameter for any particular value of h is quite significant (fig.12).

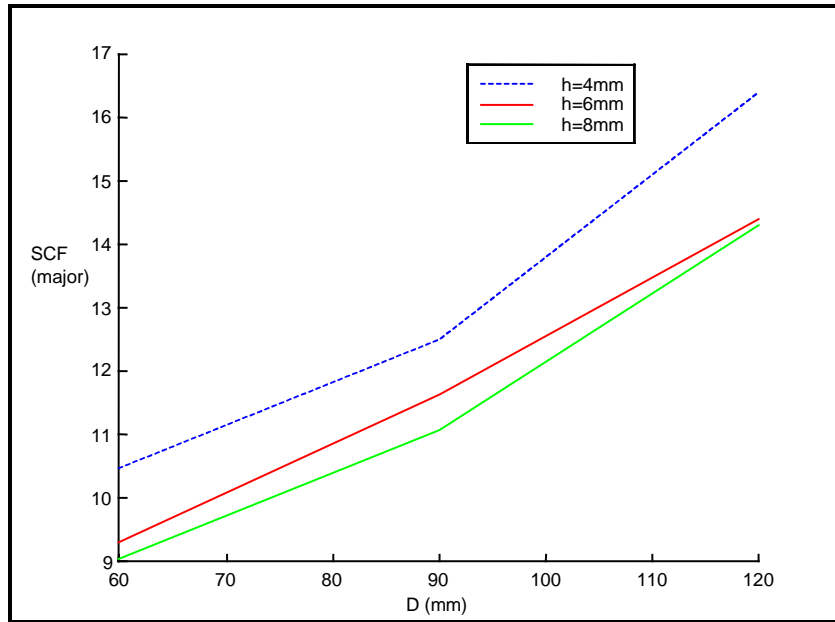


Fig. 12. Variation of maximum SCF with D and h for the Composite Rib with the flanged hole

BLF: It is clear from table 8, that as we increase the value of h , the absolute value of BLF also goes up for any cutout diameter. But the increase is not high. The variation of BLF with h for any particular cutout diameter is non-linear while the variation of BLF with the variation in cutout diameter for any particular h is fairly linear. Fig. 13 shows the variation of BLF for the various configurations chosen for their first buckling mode.

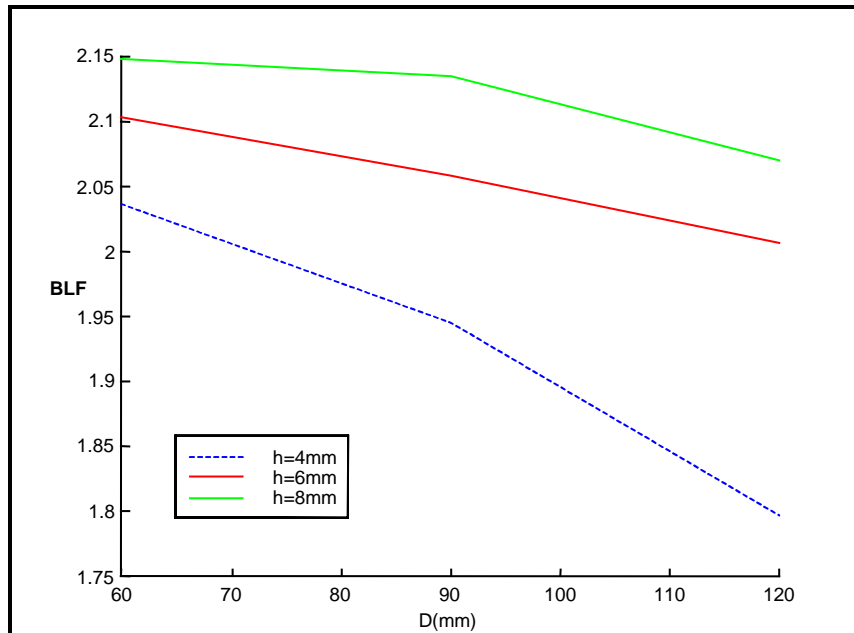


Fig. 13. Buckling Load Factors for various configurations of composite rib

Table 8. First four BLF values for various cutout size of the Composite Rib
(Shear Flow of 20 N/mm)

Sl. No.	D (mm)	h (mm)	Reinforcement Ratio (μ)	BLF			
				1	2	3	4
1	60	4	0.612	2.036	2.408	-2.507	-3.079
2	60	6	0.746	2.102	2.426	-2.597	-3.104
3	60	8	0.868	2.147	2.432	-2.666	-3.113
4	90	4	0.430	1.944	-2.297	2.473	-3.098
5	90	6	0.531	2.058	-2.425	2.563	-3.221
6	90	8	0.627	2.134	-2.520	2.610	-3.289
7	120	4	0.330	1.797	-2.035	2.395	2.684
8	120	6	0.411	2.006	-2.251	2.635	2.484
9	120	8	0.488	2.070	-2.314	2.740	3.063

Equivalent Weight Configuration: Studies are further carried out for an aluminum rib of the same weight of the composite rib with $D = 120$ mm and $h = 8$ mm (scheme 9 from table. 8 for composite rib). The studies indicate that the SCF and BLF for composite rib are 14.30 and 2.07 as compared to 8.55 and 0.827 for isotropic rib configuration for the same weight. Comparison of SCF and BLF for a) a 16 ply composite plate and b) aluminum plate of the same weight as the composite plate show significant dividends in stress and buckling loads.

Conclusions:

The SCF in the case of composite plate is higher than the corresponding value for isotropic plate. However, the allowables are higher in the case of composites. Substantial gains can be had in shear-buckling loads by the addition of flanges with the holes. Increasing the flange height leads to increase in buckling loads. Larger the cutout size, larger is the SCF. If the flange height chosen is around 8mm, the BLF remains almost constant for all the hole sizes considered. Dividends in BLF got from the addition of lip, is not very significant. However, the lip is needed from the point of view of ease of manufacture. Comparison of SCF and BLF for a) a 16 ply composite plate and b) aluminum plate of the same weight as the composite plate show significant dividends in stress and buckling loads. It is possible to go in for composite ribs with flanged cutouts leading to weight savings. Future studies are needed to be undertaken to address issues on stacking sequence, fiber orientation of plies, flange inclination, post-buckling strengths and different hole shapes. The versatility of MSC.Nastran in the analysis of composite structures enables the designers to explore new designs using composite materials.

Acknowledgements:

We wish to thank Dr. MSS Prabhu, Senior Vice President, Engineering Services Consultancy Practice Unit (ESCP) and Mr. M.R. Ravishankar, Business Manager, ESCP, of Infosys Technologies Ltd. for encouragement in promoting research and development activity along with the ongoing project execution activities of the CAE Group.

References:

1. Timoshenko, S.P., and Goodier, J. N., *Theory of Elasticity*, Third Edition, McGraw Hill Book Company, 1970.
2. Lekhnitskii, S.G., *Anisotropic Plates*, Gordon & Breach Science Publishers, 1968.
3. Liessa, A.W., *Buckling of laminated composite plates and shell panels*, Report AFWAL-TR-85-3069, June 1985.
4. *MSC.Nastran User's Manual*, Version 70.7, MSC.Software Corporation, Los-Angeles, CA.